Tomographic reconstruction for three-photon imaging

Art & Science - INPACT

13/02/2024

Mehdi Latif[1,2], Jérôme Idier[1], Thomas Carlier[2], Simon Stute[2]

[1]SiMS,LS2N - Ecole Centrale Nantes,
[2]Nuclear Oncology, CRCI[2]NA - CHU de Nantes

My thesis is about Signal & Image Processing (SIP) ...

Tomographic reconstruction for three-photon (3γ) imaging

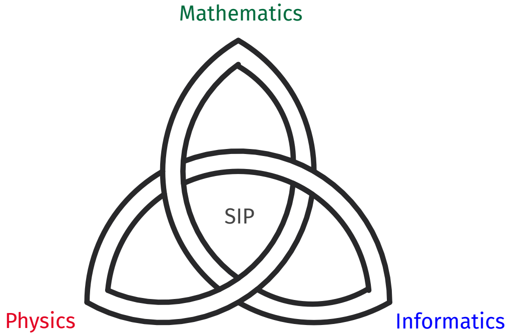

Inspired by P. Flandrin, shared by B. Pascal

What's SIP ?

- **Physics:** to describe the observed phenomena;
- **Mathematics:** to model the observed phenomena;
- **Informatics:** to implement efficient algorithms & simulate observed phenomena.

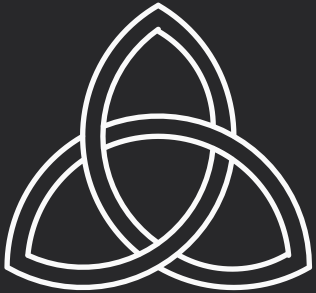

Physics

To describe the observed phenomena

The origin: XEnon Medical Imaging System (XEMIS)

Project start-up: 2004 by XENON team - Subatech laboratory (Nantes, France).

XEMIS - Grignon et al. [2007]

Low-activity medical imaging

- Development of the **Compton camera** with **liquid xenon** (LXe);
- Based on the **three-photon** (3γ) imaging technique

$\rightsquigarrow$ A camera **like no other** !!

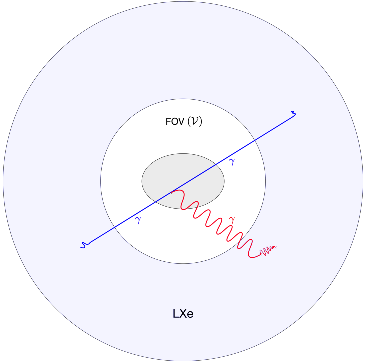

3γ **imaging** technique in XEMIS LXe **continuous** detector.

The origin: XEnon Medical Imaging System (XEMIS)

Project start-up: 2004 by XENON team - Subatech laboratory (Nantes, France).

XEMIS - Grignon et al. [2007]

Low-activity medical imaging

Development of the **Compton camera** with **liquid xenon** (LXe);

Based on the **three-photon** (3γ) imaging technique

⇝ A camera **like no other** !!

XEMIS2 - Gallego Manzano [2016]

LXe **cylindrical** & **pre-clinical** camera
for rodents **total-body** imaging

Up to now ...

Efforts are spent in experimental design of the camera.

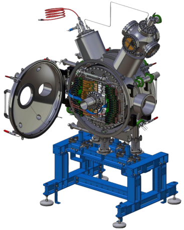

XEMIS2 sketch[1]

XEMIS2 camera - CHU-CIMA Nantes[1]

[1] **Source:** Subatech laboratory.

3γ **imaging:** a **Functional** imaging method

Injection of a radiotracer + isotope $\rightsquigarrow$ an **image** of the **radioactive distribution** in tissues.
Based on the combination of **two existing** imaging techniques & a **specific** isotope:

$$^{44}_{21}\mathrm{Sc} \xrightarrow{\beta^+} {}^{44}_{20}\mathrm{Ca}^* + \nu_e + e^+$$

$$^{44}_{20}\mathrm{Ca}^* \xrightarrow{\gamma} {}^{44}_{20}\mathrm{Ca} + \gamma \quad \text{with } E_0 = 1.157\mathrm{MeV}.$$

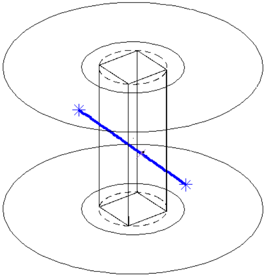

PET imaging $\rightsquigarrow$ $M^{PR} \in$ LOR

$\mathcal{L} := (V_1, V_2)$

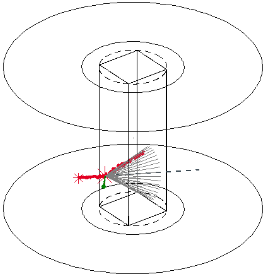

Compton imaging $\rightsquigarrow$ M $\in$ COR

$\mathcal{C} := (V_1', \overrightarrow{V_2' V_1'}, \beta)$ & $\beta = f(E_0, E_1)$

3γ **imaging:** a **Functional** imaging method

Injection of a radiotracer + isotope $\rightsquigarrow$ an **image** of the **radioactive distribution** in tissues.

Based on the combination of **two existing** imaging techniques & a **specific** isotope:

$$^{44}_{21}\mathrm{Sc} \xrightarrow{\beta^+} {}^{44}_{20}\mathrm{Ca}^* + \nu_e + e^+$$

with $E_0 = 1.157\mathrm{MeV}$.

$$^{44}_{20}\mathrm{Ca}^* \xrightarrow{\gamma} {}^{44}_{20}\mathrm{Ca} + \gamma$$

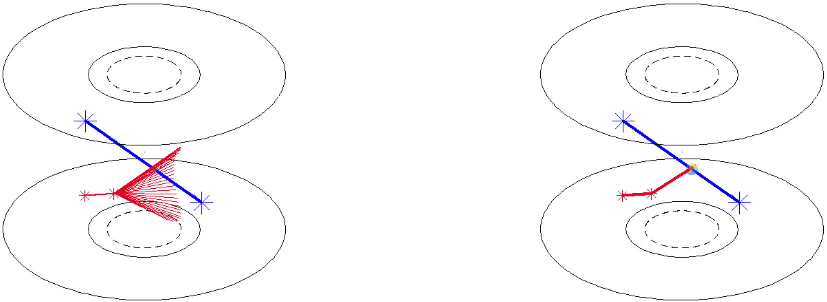

$\rightsquigarrow$ The source of the radioactive decay is **close** to the LOR/COR intersection.

Classes of detections

XEMIS2 has been developed to detect 3γ emissions - Gallego Manzano [2016].

But there's more ...

Classes of detection:

Complete detections

3γ : $2\times$ 1γ @ 511 keV and $1\times$ 1γ @ 1.157 meV;

⇝ The origin of the decay is **close** to the LOR/COR intersection.

Partial detections

$1\gamma^{511}_{\text{COR}}$: $1\times$ 1γ @ 511 keV;

$1\gamma^{1157}_{\text{COR}}$: $1\times$ 1γ @ 1.157 meV;

$2\gamma_{\text{LOR}}$: $2\times$ 1γ @ 511 keV;

$2\gamma_{\text{COR}}$: $1\times$ 1γ @ 511 keV and $1\times$ 1γ @ 1.157 meV.

⇝ the **restriction of the origin** to LOR, COR or COR could **be useful** too ...especially for **low-activity** imaging.

⇝ **Partial detection** classes are the **most detected** events ...

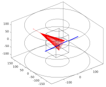

Class 3γ

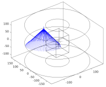

Class $1\gamma^{511}_{\text{COR}}$

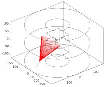

Class $1\gamma^{1157}_{\text{COR}}$

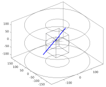

Class $2\gamma_{\text{LOR}}$

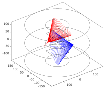

Class $2\gamma_{\text{COR}}$

XEMIS2 has been developed to detect 3γ emissions - Gallego Manzano [2016].
But there's more ...

Classes of detection:

Complete detections

3γ : $2\times$ 1γ @ 511 keV and $1\times$ 1γ @ 1.157 meV;

⇝ The origin of the decay is **close** to the LOR/COR intersection.

Partial detections

$1\gamma^{511}_{\mathrm{COR}}$: $1\times$ 1γ @ 511 keV;

$1\gamma^{1157}_{\mathrm{COR}}$: $1\times$ 1γ @ 1.157 meV;

$2\gamma_{\mathrm{LOR}}$: $2\times$ 1γ @ 511 keV;

$2\gamma_{\mathrm{COR}}$: $1\times$ 1γ @ 511 keV and $1\times$ 1γ @ 1.157 meV.

⇝ the **restriction of the origin** to LOR, COR or COR could **be useful** too ...especially for **low-activity** imaging.

⇝ **Partial detection** classes are the **most detected** events ...

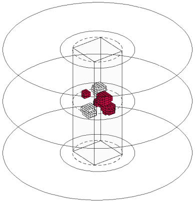

Pollux simulation: 1e+7 3γ emissions in a phantom.

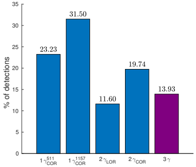

Pollux simulation: Among the ≈69% of emissions detected..

The aim of my research

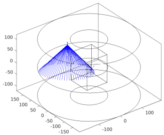

$1\gamma^{511}_{\text{COR}} \sim$ 23%

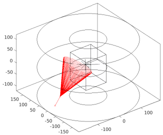

$1\gamma^{1157}_{\text{COR}} \sim$ 32%

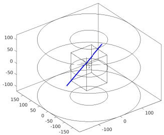

$2\gamma_{\text{LOR}} \sim$ 12%

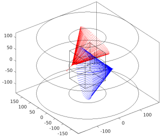

$2\gamma_{\text{COR}} \sim$ 20%

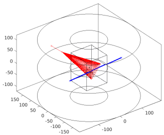

$3\gamma \sim$ 14%

Our approach to solve 3γ image reconstruction: **Anything goes... partial detections too !!**

Implement a **reconstruction framework** for 3γ imaging for XEMIS2 dealing with:

continuous LXe detection medium & multiple classes of detections

$\rightsquigarrow$ potentially suitable for other Hybrid PET/Compton camera prototypes - Llosá and Rafecas [2023].

Mathematics

To model the observed phenomena

Tomography:

From **Ancient Greek**:

τόμος (tomos) *"slice, section"* & γράφω (graphō) *"to write, describe"*

⇝ Reconstruct the volume of an object from a sequence of measurements from outside the object.

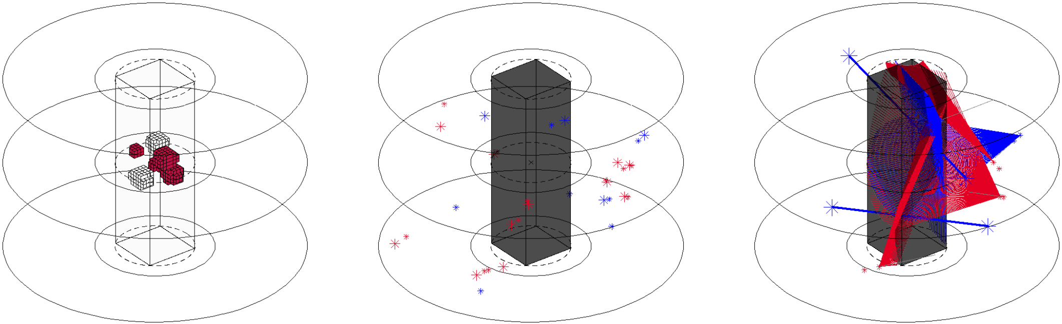

⇝ Reconstruct an image of the radioactive distribution in the tissue from the photons detected by the camera.

Tomographic reconstruction as an inverse problem

Notations: $J :=$ **Card**(voxels), $K :=$ **Card**(class), $N :=$ **Card**(detections) with $N = \sum_k N^k$.

Tomographic reconstruction $\equiv$ inverse problem

Given a collection of detections : $\boldsymbol{y} := \{\boldsymbol{y}_n\}_{n \in [\![1,N]\!]}$;

Estimate the radioactive density: $\boldsymbol{\lambda} := (\lambda_j)_{j \in [\![1,J]\!]}$.

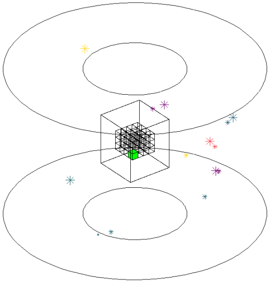

Direct model:

To link $\boldsymbol{y}$ and $\boldsymbol{\lambda}$:

$$\boldsymbol{y} := \bigcup_{k=1}^{K} \left\{\boldsymbol{y}_n^k\right\}_{n \in [\![1,N^k]\!]} \quad \text{iid} \quad y_n^k \sim \mathcal{P}\left(\bar{\boldsymbol{y}}^k\right)$$

where:

$$\bar{\boldsymbol{y}}^k := \sum_{j=1}^{J} T_j^k(\boldsymbol{y}^k)\lambda_j + \bar{\varepsilon}^k \quad \forall n \in [\![1, N_k]\!] \quad \forall k \in [\![1, K]\!].$$

Complex problem:

$\Rightarrow$ Large dimensions of $\mathbf{T} \xrightarrow{\bar{\varepsilon}^k=0} \cancel{\mathbf{T}^{-1}}$;

$\Rightarrow$ perturbated measurement vector $\boldsymbol{y}$;

$\Rightarrow$ Small perturbation in projection space $\rightsquigarrow$ Large error in image space.

Expectation–Maximization algorithm

$$\hat{\boldsymbol{\lambda}}^{\mathrm{ML}} = \underset{\boldsymbol{\lambda}\in\mathbb{R}_+^J}{\mathrm{argmax}} \;\log L(\boldsymbol{\lambda}|\boldsymbol{y})$$

Expectation–Maximization (EM) algorithm - Dempster et al. [1977]

Determine $\widehat{\boldsymbol{\lambda}}^{\mathrm{ML}}$ for a probabilistic model depending on **hidden data**:

$\boldsymbol{y} := \{\boldsymbol{y}_n\}_{n\in[\![1,N]\!]}$ are **known** ,$\boldsymbol{z} := \{\boldsymbol{z}_{n,j}\}_{n\in[\![1,N]\!],j\in[\![1,J]\!]}$ are **hidden** $\rightsquigarrow$ $(\boldsymbol{y},\boldsymbol{z})$ are the **complete** data.

$\rightsquigarrow$ $\boldsymbol{z}$ is not accessible, but we can **estimate it !!**

The EM recipe:

Starting from an initial guess $\hat{\boldsymbol{\lambda}}^0$:

E-Step: define the auxiliary function with $\hat{\boldsymbol{\lambda}}^0$:

$$Q\left(\boldsymbol{\lambda}|\hat{\boldsymbol{\lambda}}^0\right) := \mathbb{E}_{\boldsymbol{z}|\hat{\boldsymbol{\lambda}}^0}\left(\log p(\boldsymbol{y},\boldsymbol{z}\mid\boldsymbol{\lambda})\right)$$

M-Step: Get a better estimate $\hat{\boldsymbol{\lambda}}^1$:

$$\hat{\boldsymbol{\lambda}}^1 := \underset{\boldsymbol{\lambda}\in\mathbb{R}_+^J}{\mathrm{argmax}}\, Q\left(\boldsymbol{\lambda}|\hat{\boldsymbol{\lambda}}^0\right)$$

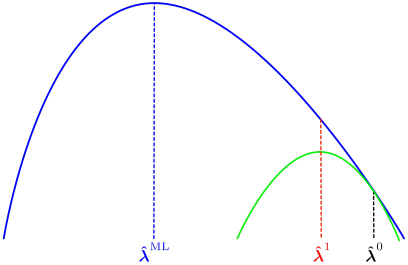

EM convergence scheme for Poisson $\log L(\boldsymbol{\lambda}|\boldsymbol{y})$
Inspired by A.J.Reader

$$\hat{\boldsymbol{\lambda}}^{\text{ML}} = \underset{\boldsymbol{\lambda}\in\mathbb{R}_+^J}{\text{argmax}} \ \log L(\boldsymbol{\lambda}|\boldsymbol{y})$$

Expectation–Maximization (EM) algorithm - Dempster et al. [1977]

Determine $\widehat{\boldsymbol{\lambda}}^{\text{ML}}$ for a probabilistic model depending on **hidden data**:

$\boldsymbol{y} := \{\boldsymbol{y}_n\}_{n\in[\![1,N]\!]}$ are **known** ,$\boldsymbol{z} := \{\boldsymbol{z}_{n,j}\}_{n\in[\![1,N]\!],j\in[\![1,J]\!]}$ are **hidden** $\rightsquigarrow$ $(\boldsymbol{y},\boldsymbol{z})$ are the **complete** data.

$\rightsquigarrow$ $\boldsymbol{z}$ is not accessible, but we can **estimate it !!**

The EM recipe:

Starting from the new guess $\hat{\boldsymbol{\lambda}}^1$:

E-Step: define the auxiliary function with $\hat{\boldsymbol{\lambda}}^1$:

$$Q\left(\boldsymbol{\lambda}|\hat{\boldsymbol{\lambda}}^1\right) := \mathbb{E}_{\boldsymbol{z}|\hat{\boldsymbol{\lambda}}^1}\left(\log p(\boldsymbol{y},\boldsymbol{z} \mid \boldsymbol{\lambda})\right)$$

M-Step: Get a better estimate $\hat{\boldsymbol{\lambda}}^2$:

$$\hat{\boldsymbol{\lambda}}^2 := \underset{\boldsymbol{\lambda}\in\mathbb{R}_+^J}{\text{argmax}}\, Q\left(\boldsymbol{\lambda}|\hat{\boldsymbol{\lambda}}^1\right)$$

and repeat both steps until the convergence to $\hat{\boldsymbol{\lambda}}^{\text{ML}}$

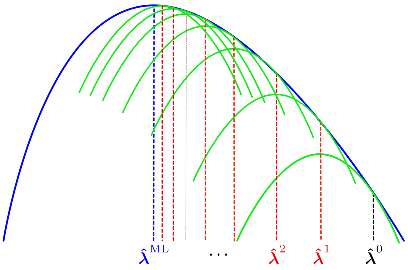

EM convergence scheme for Poisson $\log L(\boldsymbol{\lambda}|\boldsymbol{y})$
Inspired by A.J.Reader

$$\hat{\boldsymbol{\lambda}}^{\mathrm{ML}} = \underset{\boldsymbol{\lambda}\in\mathbb{R}_+^J}{\mathrm{argmax}} \; \log L(\boldsymbol{\lambda}|\boldsymbol{y})$$

MC-LM-MLEM - Latif et al. [2023a]

Proof of the extension of LM-MLEM proposed for PET & Compton imaging - Parra and Barrett [1998]; Wilderman et al. [1998a].

$$\begin{cases} \hat{\boldsymbol{\lambda}}^{(0)} = \hat{\lambda}_j^{(0)} > 0 \\ \hat{\lambda}_j^{(t+1)} := \hat{\lambda}_j^{(t)} \times \underbrace{\frac{1}{\sum_k s_j^k} \sum_{k=1}^{K} \sum_{n=1}^{N^k} \frac{T_j^k(\boldsymbol{y}_n^k)}{\sum_{j'} T_{j'}^k(\boldsymbol{y}_n^k)\hat{\lambda}_{j'}^{(t)} + \bar{\varepsilon}_n^k}}_{\text{Correction factor}} \quad \forall j \in [\![1, J]\!] \end{cases}$$

Property:

The algorithm converges to a $\hat{\boldsymbol{\lambda}}^{\mathrm{ML}}$ with non-negative densities ...

Class dependant terms !!

- $T_j^k(\boldsymbol{y}_n^k)$: the **system "matrix"** of class k at voxel j computed **on the fly**;
- s_j^k: the **sensitivity** of class k at voxel j, which is **pre-computed**:

$$s_j^k := \int_{\omega\in\Omega^k} T_j^k(\omega)\mathrm{d}\omega$$

Computer science

To implement efficient algorithms & simulate observed phenomena

Sensitivity vector s^k

The **sensitivity** of class k which is **pre-computed**:

$$\boldsymbol{s}^k = \left(s_j^k\right)_{j\in[\![1,J]\!]} \quad \text{with} \quad s_j^k := \int_{\omega\in\Omega^k} T_j^k(\omega)\mathrm{d}\omega \quad \forall k \in [\![1,K]\!].$$

LOR based classes:

Let M be an emission point of an annihilation belonging to the voxel j in the FOV $\mathcal{V}$:

$$\begin{aligned} s_j^{\mathrm{LOR}}(M) := \int_{\theta=0}^{\pi} \Bigg[& \int_{\varphi=0}^{\frac{\pi}{2}} p_i\left(\frac{1}{|\cos(\varphi)|}\left(\sqrt{R_{\mathrm{out}}^{2\gamma}(\varphi, I1)^2 - \tilde{O}P^2} - Q\right)\right) \times p_i\left(\frac{1}{|\cos(\varphi)|}\left(\sqrt{R_{\mathrm{out}}^{2\gamma}(\varphi, J2)^2 - \tilde{O}P^2} - Q\right)\right)\mathrm{d}\varphi \\ & + \int_{\varphi=-\frac{\pi}{2}}^{0} p_i\left(\frac{1}{|\cos(\varphi)|}\left(\sqrt{R_{\mathrm{out}}^{2\gamma}(\varphi, I2)^2 - \tilde{O}P^2} - Q\right)\right) \times p_i\left(\frac{1}{|\cos(\varphi)|}\left(\sqrt{R_{\mathrm{out}}^{2\gamma}(\varphi, J1)^2 - \tilde{O}P^2} - Q\right)\right)\mathrm{d}\varphi\Bigg]\mathrm{d}\theta, \end{aligned}$$

where $\tilde{O}P := \sin(\theta)\tilde{O}M$, $Q := \sqrt{R_1^2 - \tilde{O}P^2}$.

Sensitivity vector s^k

The **sensitivity** of class k which is **pre-computed**:

$$\boldsymbol{s}^k = \left(s_j^k\right)_{j\in[\![1,J]\!]} \quad \text{with} \quad s_j^k := \int_{\omega\in\Omega^k} T_j^k(\omega)\mathrm{d}\omega \quad \forall k \in [\![1,K]\!].$$

COR based classes:

Let M be an emission point of a E_0 photon belonging to the voxel j in the FOV $\mathcal{V}$:

$$s_j^{\text{COR}}(M) := \int_{\theta=0}^{2\pi} \Bigg[\int_{\varphi=0}^{\frac{\pi}{2}} \int_{v=R_{\text{in}}}^{R_{\text{out}}^{1\gamma}(\varphi,I1)} h(\varphi,\theta,v)\mathrm{d}v\mathrm{d}\varphi + \int_{\varphi=\frac{\pi}{2}}^{\pi} \int_{v=R_{\text{in}}}^{R_{\text{out}}^{1\gamma}(\varphi,J1)} h(\varphi,\theta,v)\mathrm{d}v\mathrm{d}\varphi$$
$$+ \int_{\varphi=-\frac{\pi}{2}}^{0} \int_{v=R_{\text{in}}}^{R_{\text{out}}^{1\gamma}(\varphi,I2)} h(\varphi,\theta,v)\mathrm{d}v\mathrm{d}\varphi + \int_{\varphi=-\pi}^{-\frac{\pi}{2}} \int_{v=R_{\text{in}}}^{R_{\text{out}}^{1\gamma}(\varphi,J2)} h(\varphi,\theta,v)\mathrm{d}v\mathrm{d}\varphi \Bigg] \mathrm{d}\theta,$$

with $h(\varphi,\theta,v) := f(\varphi,\theta,v) \times C(v,\theta,\varphi)$ and

$$f(\varphi,\theta,v) := p_i \left(\frac{1}{|\cos(\varphi)|} \left(\sqrt{v^2 - \sin^2(\theta)\tilde{O}M^2} - \sqrt{R_{\text{in}}^2 - \sin^2(\theta)\tilde{O}M^2} \right) \right)$$

$$C(v,\theta,\varphi) := \int_{\beta=0}^{\pi} K(\beta|E_0) \int_{\omega=0}^{2\pi} \int_{\rho=0}^{\rho_{\max}(v,\theta,\varphi,\beta,\omega)} p_i'\left(\|\overrightarrow{V_1V_2}\|_2\right)\mathrm{d}\beta\mathrm{d}\omega\mathrm{d}\rho$$

$\rightsquigarrow$ A bit complicated to evaluate analytically, **but** useful for Pollux development.

Sensitivity vector s^k - approximation through Monte Carlo simulation

Pollux simulation to get $\hat{s}^k$:

FOV $\mathcal{V}$ dimensions: 70×70×240 mm

Discretization of $\mathcal{V}$ into 14×14×24 voxels of size 5×5×10 mm;

For each voxel : 3e+6 uniformly generated 3γ emissions.

$\rightsquigarrow$ *For each 3γ emission, which class k is detected?*

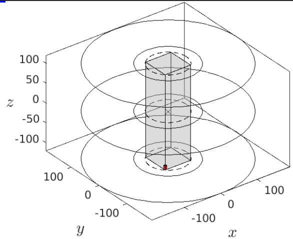

Results (after a few days)

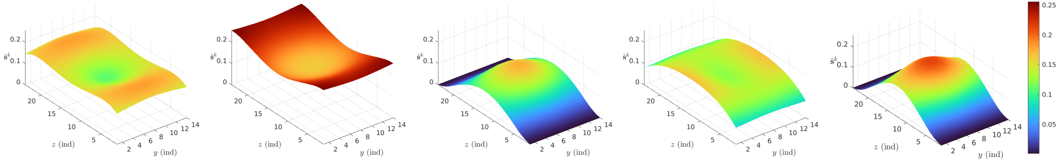

$1\gamma^{511}_{\text{COR}}$ $1\gamma^{1157}_{\text{COR}}$ $2\gamma_{\text{LOR}}$ $2\gamma_{\text{COR}}$ 3γ

Visually: the classes are **spatially complementary** *e.g.*, in the center & at the edges of $\mathcal{V}$;

Really informative? Multi-class Fisher information matrix - Latif et al. [2023b] $\rightsquigarrow$ $T^k(.)$ is **required**!

System matrix at glance

$$T_j^k(\boldsymbol{y}^k) := P^k(\boldsymbol{y}^k) A_j^k(\boldsymbol{y}^k) \quad \forall k \in [\![1, K]\!], \forall j \in [\![1, J]\!],$$

where:

$P^k(.)$ relates to the **path of the photon** in the detector **& independent** of voxels J.

$A_j^k(.)$ is the **projector** which links **image space** (J voxels) ⟳ **data space** (N detections).

PET imaging ⇝ LOR

$A_j^k(.) \propto$ length$(\mathcal{L} \cap v_j)$ - Siddon [1985]

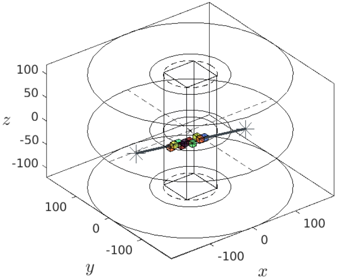

Compton imaging ⇝ COR

$A_j^k(.) \propto$ angular dist$(\mathcal{C}(V_1, \overrightarrow{V_2V_1}, \beta), v_j)$

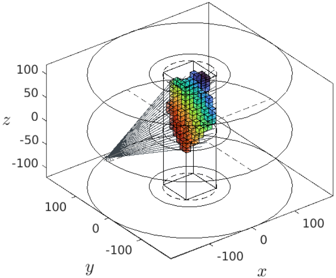

⇝ Estimating $A_j^k(.)$ is **quite simple** with **PET** imaging, but a **bit harder** for **Compton** imaging.

System matrix for Compton imaging: state-of-the-art

$$T_j^k(\boldsymbol{y}^k) \propto A_j^k(\boldsymbol{y}^k) := \int_{M \in v_j \cap \mathcal{C}} f_\beta(M) \mathrm{d}v$$

⇝ Surface integral on $M \in v_j \cap \mathcal{C}$, a bit complicated to evaluate analytically ...

State-of-the-art: Cone-driven methods for system matrix approximation:

Ellipse-stacking method (ESM)
Wilderman et al. [1998b]

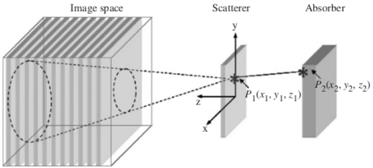

Ray-tracing method (RTM)
Kim et al. [2007], Siddon [1985]

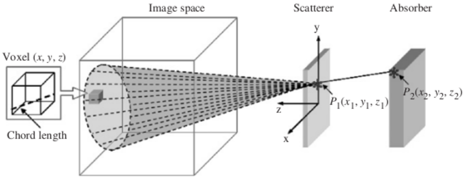

- According to Kim et al. [2007], RTM $\gg$ ESM for reconstructed image quality ... sampling conditions ?

⚠ Energy uncertainties ⇝ Shell of Response (SOR)

$$\cos\beta := 1 - \frac{m_e c^2 E_1}{E_0(E_0 - E_1)} \Longrightarrow \mathcal{S}(V_1, \overrightarrow{V_2V_1}, \tilde{\beta}, \delta\beta) := \left\{\beta \in [\tilde{\beta} - \delta\beta; \tilde{\beta} + \delta\beta] \mid \mathcal{C}(V_1, \overrightarrow{V_2V_1}, \beta)\right\}$$

- A **hybrid** ESM/RTM approach was proposed - Lojacono [2013], **but** the results were inconclusive ...

System matrix for Compton imaging: our approach !

$$T_j^k(\boldsymbol{y}^k) \propto A_j^k(\boldsymbol{y}^k) := \int_{M \in v_j \cap \mathcal{S}} f_\beta(M)\mathrm{d}v$$

Volume integral on $M \in v_j \cap \mathcal{S}$ due to energy uncertainty $\rightsquigarrow$ a bit complicated to evaluate analytically ...

LS2N/CRCI^{2}NA method: Voxel-driven methods for system matrix approximation ($\neq$ Cone-driven)

$\rightsquigarrow$ A two-step approach using cubic voxel $v_j \in \mathcal{V}$:

Step 1: Conic section screening

To find all voxels st. $v_j \cap \mathcal{S} \neq \emptyset$

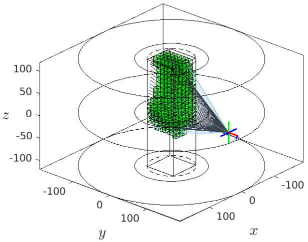

Step 2: Voxel deformation $\breve{v}_j$ preserving vol(v_j)

To easily compute an approximation of vol$(v_j \cap \mathcal{S})$.

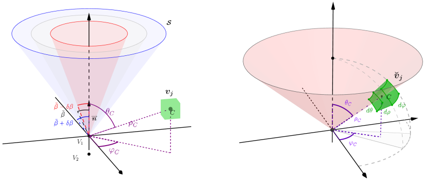

(a) Spherical coordinates **(b)** Spherical box

$\rightsquigarrow$ **Approximation for non-degenerate $\breve{v}$:** $\breve{A}_j(\boldsymbol{y}) = \left(\rho_C^2 + \frac{d^2}{12}\right) \times \frac{d^2}{\rho_C\sqrt{\sin(\theta_C)}} \times I_{\tilde{\beta}}(\theta \mid \Theta_{\mathcal{S}}(\breve{v}_j), \delta\beta)$

What’s next ?

What's next ?

Mathematics

- Handle pathological cases for the evaluation of $T_j^k(.)$ in Compton imaging, *aka. Galipeurs*;
- Ill-posed problem $\oplus$ Low-activity imaging ... some *a priori* knowledge on $\boldsymbol{\lambda}$ can be helpful;
  $\rightsquigarrow$ to implement a regularization method for the MC-LM-MLEM algorithm - De Pierro [1995]

Informatics

- Using Pollux simulations, to implement our new methods in the CASToR framework - Merlin et al. [2018].

Physics

- Implement energy uncertainty in Pollux simulations - Gallego Manzano [2016];
- Use more realistic detections generated by the GEANT4 framework - Agostinelli et al. [2003].

Other

- Writing my PhD thesis manuscript ...
- a paper about *Voxel-driven method for system matrix evaluation in Compton imaging* ...

Thank you for your attention

Questions ?

Agostinelli, S., Allison, J., and ... (2003). Geant4—a simulation toolkit. Nuclear Instruments and Methods in Physics Research Section A: Accelerators, Spectrometers, Detectors and Associated Equipment, 506(3):250–303.

De Pierro, A. (1995). A modified expectation maximization algorithm for penalized likelihood estimation in emission tomography. IEEE Trans. Med. Imag., 14(1):132–137.

Dempster, A. P., Laird, N. M., and Rubin, D. B. (1977). Maximum likelihood from incomplete data via the *EM* algorithm. 39(1):1–22.

Gallego Manzano, L. (2016). Optimization of a single-phase liquid xenon Compton camera for 3γ medical imaging. Theses, Ecole des Mines de Nantes.

Grignon, C., Barbet, J., Bardiès, M., Carlier, T., Chatal, J., Couturier, O., Cussonneau, J., Faivre, A., Ferrer, L., Girault, S., Haruyama, T., Le Ray, P., Luquin, L., Lupone, S., Métivier, V., Morteau, E., Servagent, N., and Thers, D. (2007). Nuclear medical imaging using β^+, γ coincidences from 44Sc radio-nuclide with liquid xenon as detection medium. NIM-A, 571(1-2):142–145.

Kim, S. M., Lee, J. S., Lee, M. N., Lee, J. H., Lee, C. S., Kim, C.-H., Lee, D. S., and Lee, S.-J. (2007). Two approaches to implementing projector–backprojector pairs for 3d reconstruction from compton scattered data. Nuclear Instruments and Methods in Physics Research Section A: Accelerators, Spectrometers, Detectors and Associated Equipment, 571(1):255–258. Proceedings of the 1st International Conference on Molecular Imaging Technology.

Latif, M., Idier, J., Carlier, T., and Stute, S. (2023a). Multi-class maximum likelihood expectation-maximization list-mode image reconstruction. In International Meeting on Fully Three-Dimensional Image Reconstruction in Radiology and Nuclear Medicine (Fully3D 2023), Stony Brook, United States.

Latif, M., Idier, J., Carlier, T., and Stute, S. (2023b). Reconstruction multiclasse pour l'imagerie TEP 3-photons. In GRETSI'23, Grenoble, France. Groupe de Recherche et d'Etudes de Traitement du Signal et des Images.

Llosá, G. and Rafecas, M. (2023). Hybrid PET/Compton-camera imaging: an imager for the next generation. The European Physical Journal Plus, 138(3):214.

Lojacono, X. (2013). Image reconstruction for Compton camera with application to hadrontherapy. Theses, INSA de Lyon.

Merlin, T., Stute, S., Benoit, D., Bert, J., Carlier, T., Comtat, C., Filipovic, M., Lamare, F., and Visvikis, D. (2018). CASToR: a generic data organization and processing code framework for multi-modal and multi-dimensional tomographic reconstruction. Phys. Med. Biol., 63(18):185005.

Parra, L. and Barrett, H. (1998). List-mode likelihood: EM algorithm and image quality estimation demonstrated on 2-D PET. IEEE Trans. Med. Imag., 17(2):228–235.

Siddon, R. L. (1985). Fast calculation of the exact radiological path for a three?dimensional ct array. Medical Physics, 12(2):252–255.

Wilderman, S., Clinthorne, N., Fessler, J., and Rogers, W. (1998a). List-mode maximum likelihood reconstruction of compton scatter camera images in nuclear medicine. In 1998 IEEE NSS/MIC, pages 1716–1720.

Wilderman, S., Rogers, W., Knoll, G., and Engdahl, J. (1998b). Fast algorithm for list mode back-projection of Compton scatter camera data. IEEE Transactions on Nuclear Science, 45(3):957–962.